RSC Advances

RSC Publishing

COMMUNICATION

View Article Online
View Journal

High surface area metal salt templated carbon aerogels *via* a simple subcritical drying route: preparation and CO_2 uptake properties†

Cite this: DOI: 10.1039/c3ra43420f

Received 5th July 2013,
Accepted 26th July 2013

DOI: 10.1039/c3ra43420f

www.rsc.org/advances

Eric Masika and Robert Mokaya*

We describe a very simple method for the formation of high surface area carbon aerogels from melamine–formaldehyde resins, *via* metal salt ($CaCl_2$) templating, wherein subcritical drying is used and no activation is required. The metal salt acts as a porogen to generate carbon aerogels with surface area of up to 1100 m^2 g^{-1}, which exhibit significant CO_2 uptake of up to 2.2 mmol g^{-1} at 298 K and 1 bar.

A number of classes of porous materials such as carbons and metal organic frameworks (MOFs) are considered as possible candidates for energy related applications (*e.g.*, gas storage).[1–4] Porous carbons are attractive due to their chemical inertness, stability under various environments, versatility and low density, and are currently under intense investigation for potential applications in gas storage.[1,4] More generally, an important research theme in porous carbon synthesis is the development of simpler and cheaper preparation routes to carbons with attractive textural properties. Carbon aerogels are of interest due to their low bulk density and a high internal surface area. Carbon aerogels are conventionally synthesized *via* three sequential steps; (i) sol–gel polymerization of molecular precursors into an organic gel, (ii) drying of the organic gel and (iii) carbonization of the organic gel to generate the final carbon aerogel. A particular disadvantage of the conventional method of generating carbon aerogels is that the organic gels typically require supercritical drying[5] or freeze-drying[6] prior to carbonization to the final carbon aerogel. Usually the carbon aerogel is then activated in order to generate a high surface area carbon.[7]

The special drying conditions (supercritical or freeze drying) are considered essential for the retention of porosity in the organic gels;[8] conventional air-drying generally leads to collapse of the organic gel network, which precludes the formation of a high surface area carbon after carbonization. However, the use of specialised drying techniques is cumbersome and requires specialised equipment, and therefore it is desirable to develop simpler synthesis routes to carbon aerogels. It would also be simpler to generate high surface area carbon aerogels without the need for the activation process. In this regard, templates of various forms have been widely used for the preparation of porous carbons.[9] The templates are usually needed to either generate porosity or to cause structural ordering in the templated carbons.[9] Whilst structural order is not a requirement for carbon aerogels, there is scope for the use of templates to generate porosity in a way that may negate the need for activation. Here we report on a very simple route that employs the use of a metal salt template for the formation of carbon aerogels wherein, additionally, subcritical drying is used and no activation is required to generate high surface area. Furthermore, no extra steps are required during the subcritical drying process.[10]

Briefly (see ESI† for details), 4.2 g of melamine and 19.4 g of 37% formaldehyde were added to 15 ml of water under stirring, followed by the addition of 0.44 g of 0.1 M sodium carbonate solution. The resulting mixture with a pH of 8.5 was heated at 40 °C until a clear solution of hexamethylomelamine (MF) was formed after which metal salt (33.6 g of $CaCl_2$) was added at a $CaCl_2$/MF ratio of 2. The pH of the resulting solution was adjusted to 4.5 by addition of 1 M HCl and heated at 60 °C for 1 h to generate a MF resin/$CaCl_2$ composite. The composite was dried and cured at 180 °C for 6 h and then carbonised at 700, 800 or 900 °C for 2 h under nitrogen. The resulting carbon aerogels were washed with water to remove the metal salt template, and denoted as Ca-CAMFx (where x is carbonisation temperature).

The nitrogen sorption isotherms of the carbon aerogels are shown in Fig. 1 and the textural properties are summarised in Table 1. The isotherms of all three templated carbon aerogels are close to type IV and display a H4 type hysteresis loop at relative pressure (P/Po) above 0.5,[11] which is indicative of the presence of narrow slit-like pores. Templated carbon aerogels pyrolysed at 700 and 800 °C (*i.e.*, Ca-CAMF900 and Ca-CAMF800) have higher adsorption, and thus greater porosity compared to sample Ca-

School of Chemistry, University of Nottingham, University Park, NG & 2RD, Nottingham. E-mail: r.mokaya@nottingham.ac.uk; Tel: 0115 8466174

† Electronic supplementary information (ESI) available: Details of carbon aerogel synthesis and CO_2 uptake measurements. One table with textural and CO_2 uptake data for activated templated carbon aerogels. Three figures: nitrogen sorption isotherms and pore size distribution curves for activated templated carbon aerogels, and CO_2 uptake as a function of time for activated non-templated and activated templated carbon aerogels. See DOI: 10.1039/c3ra43420f

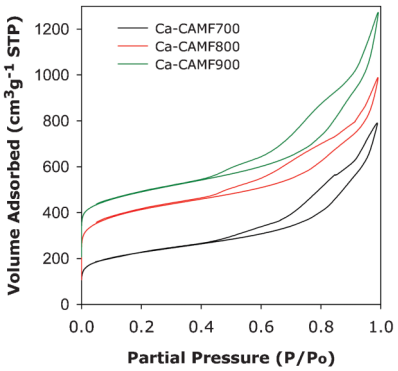

Fig. 1 Nitrogen sorption isotherms for Ca-CAMFx samples carbonised at 700, 800 or 900 °C. For clarity isotherms for Ca-CAMF800 and Ca-CAMF900 are offset (*y*-axis) by 100 and 200 $cm^3\ g^{-1}$, respectively.

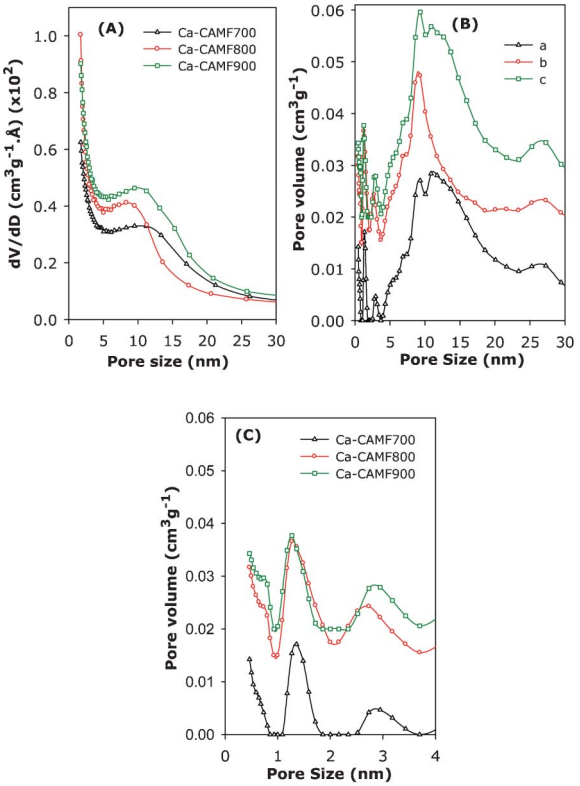

Fig. 2 Pore size distribution (PSD) curves obtained using (A) BJH or (B,C) NLDFT analysis for $CaCl_2$-templated Ca-CAMFx carbon aerogels (where x is pyrolysis temperature; 700, 800, or 900 °C); a, b and c in (B) refers to Ca-CAMF700, Ca-CAMF800 and Ca-CAMF900, respectively.

CAMF700. The surface area of the $CaCl_2$-templated carbon aerogels varies between 785 and 1090 $m^2\ g^{-1}$ and the pore volume ranges from 1.22 to 1.66 $cm^3\ g^{-1}$ as summarised in Table 1. These textural properties are amongst the highest ever reported for unactivated carbon aerogels,[12] and are by far the highest for carbon aerogels prepared *via* subcritical drying.[10] It is noteworthy that a carbon aerogel (designated as CAMF), which was prepared in a manner similar to the templated carbon aerogels but with no metal salt template, was virtually non-porous with a surface area of 4 $m^2\ g^{-1}$ and hardly any pore volume (Table 1). We therefore attribute the high surface area of the templated carbon aerogels to the positive influence of using a porogen, which in the present case is a metal salt ($CaCl_2$). The templated carbon aerogels exhibit significant microporosity, which is a contributing factor to the high total surface area observed; the proportion of surface area associated with micropores is 48%, 56% and 55% for Ca-CAMF700, Ca-CAMF800 and Ca-CAMF900, respectively, and thus relatively similar irrespective of the pyrolysis temperature. On the other hand, the proportion of micropore volume is rather lower at 14%, 20% and 13% for Ca-CAMF700, Ca-CAMF800 and Ca-CAMF900, respectively. We propose that the $CaCl_2$ acts as a porogen by generating a continuous inorganic phase within the carbon network. Dissolution of the inorganic phase then creates porosity in the carbon aerogel, which retains structural integrity following carbonisation at high temperature (700–900 °C). This proposal is supported by the fact that the carbon aerogels were found to have no porosity prior to the final washing step. The washing step, which removes the metal salt or its derivatives, is an essential step in generating porosity. The pyrolysis temperature appears to have an influence on the textural properties with the aerogel carbonised at 800 °C (Ca-CAMF800) exhibiting the highest surface area.

The pore size distribution (PSD) curves of the templated carbon aerogels are shown in Fig. 2 and the pore size data is summarised in Table 1. PSD curves obtained *via* BJH analysis (Fig. 2A) show a relatively broad distribution of pore sizes with the maximum centred at *ca.* 10 nm for Ca-CAMF700 and Ca-CAMF900 and 9 nm for Ca-CAMF800. The BJH analysis also suggests the presence of micropores, with their proportion being highest for sample Ca-CAMF800 which is consistent with the extent of microporosity (Table 1). Given the limitations of BJH analysis in probing the presence of micropores, we performed pore size analysis using the

Table 1 Textural properties and CO_2 uptake of $CaCl_2$-templated carbon aerogels

Sample	Surface area ($m^2\ g^{-1}$)[b]	Pore volume ($cm^3\ g^{-1}$)[c]	Pore size (nm)[d]	CO_2 uptake (mmol g^{-1})[ef]
CAMF[a]	4	0.01		
Ca-CAMF700	785 (375)	1.22 (0.18)	1.2/3/10	2.1 (2.7)
Ca-CAMF800	1090 (611)	1.37 (0.28)	1.2/3/9	2.2 (1.9)
Ca-CAMF900	1014 (557)	1.66 (0.21)	1.2/3/10	1.7 (1.7)

[a] CAMF is the non-templated carbon aerogel. The values in parentheses refer to. [b] Micropore surface area. [c] Micropore volume. [d] Maxima of pore size obtained from PSD curves. [e] CO_2 uptake at 298 K and 1 bar. [f] The values in parenthesis are CO_2 uptake density in μmol m^{-2}.

Table 2 Textural properties and CO_2 uptake of non-templated carbon aerogel before (CAMF) and after activation (12AC-CAMFX, where X is activation temperature) at KOH/carbon ratio = 2

Sample	Surface area (m^2 g^{-1})[b]	Pore volume (cm^3 g^{-1})[c]	Pore size (nm)[d]	CO_2 uptake (mmol g^{-1})[e]
CAMF[a]	4	0.01		
12AC-CAMF600	84 (59)	0.05 (0.03)	1.1	1.0
12AC-CAMF700	260 (203)	0.16 (0.10)	0.6/1.2	1.5
12AC-CAMF800	637 (550)	0.33 (0.26)	0.8/1.5	1.9
12AC-CAMF800	860 (736)	0.45 (0.35)	0.8/2.2	2.0

[a] CAMF is the non-templated carbon aerogel. The values in parentheses refer to. [b] Micropore surface area. [c] Micropore volume. [d] Maxima of pore size obtained from PSD curves. [e] CO_2 uptake at 298 K and 1 bar.

NLDFT model, which as shown in Fig. 2B also indicated the presence of pores of size *ca.* 10 nm for all the templated carbon aerogels. In addition, the NLDFT analysis indicated the presence of small (3 nm) and large (26 nm) mesopores (Fig. 2B) along with micropores of size 1.2 nm (Fig. 2C). Overall, though, both BJH and NLDFT pore size analysis indicate that the predominant pores are large mesopores of size *ca.* 10 nm, which is typical for carbon aerogels.[7]

As described above, the formation of the templated carbon aerogels is very simple and high surface area may be generated in the absence of supercritical drying or activation. For comparison, we activated the non-templated carbon aerogel (CAMF) and compared the properties of the resulting activated carbons (Table 2 and Fig. 3) with the metal salt templated samples. The nitrogen sorption isotherms in Fig. 3 indicate that activation of the non-templated CAMF aerogel generates some micro and meso-porosity but the overall porosity achieved is modest; the surface area of the activated CAMF carbons varies between 80 and 860 m^2 g^{-1}, with pore volume no larger than 0.45 cm^3 g^{-1}. Thus even after activation at up to 900 °C, the activated carbons derived from the non-templated carbon aerogel generally had lower surface area and pore volume compared to the metal salt templated carbon aerogels (Table 2). The pores of the activated CAMF carbons (Fig. 3) are mainly in the micropore and lower mesopore range, while metal salt templated carbons, in addition to micropores, also possess much larger mesopores (Fig. 2). This observations rather illustrates the attraction of the metal salt templating method.

On the other hand, activation of a templated carbon aerogel (*e.g.*, Ca-CAMF800) leads to a significant increase in porosity (Table S1 and Fig. S1, ESI†); according to nitrogen sorption isotherms (Fig. S1, ESI†), activation at 600 °C leads to a modest increase in nitrogen adsorption at lower relative pressure (P/Po) and an apparent loss of the large pores present in Ca-CAMF800 to generate a carbon with a type I isotherm suggesting a highly microporous nature, while activation at 800 °C results in an increase in both the microporosity and mesoporosity. The PSD of the activated templated carbon aerogels (Fig. S1, ESI†) indicate that activation at 600 °C removes the 10 nm pores present in the parent Ca-CAMF800 carbon but retains the 1.2 and 3 nm pores. A similar trend is observed for activation at 800 °C except that there is much larger increase in the proportion of pores of size *ca.* 3 nm. Overall, therefore the activation of the $CaCl_2$-templated carbon aerogels shifts the porosity towards smaller pores. The activated templated carbon aerogels have high surface area of up to 3343 m^2 g^{-1} representing an increase of >200% over the parent Ca-CAMF800 aerogel (Table S1, ESI†). The pore volume reduces for the sample activated at 600 °C, which is consistent with the shift to microporosity as discussed above, and then increases for the sample activated at 800 °C to reach the extraordinarily large value of 2.65 cm^3 g^{-1}(Table S1, ESI†).

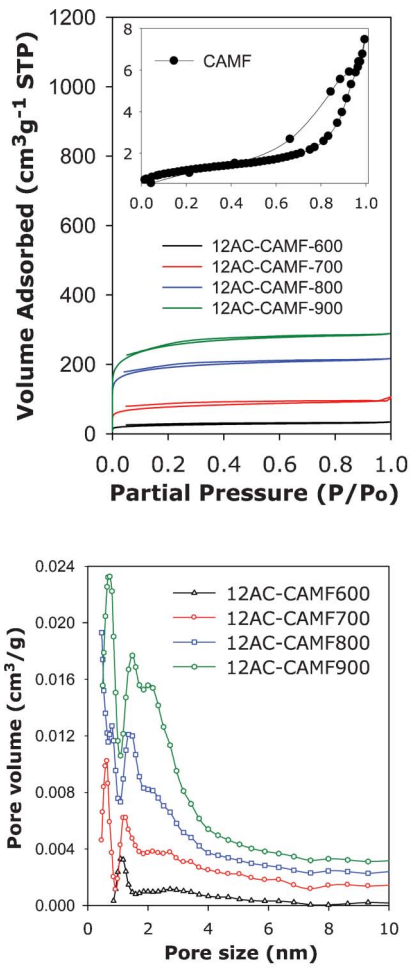

Fig. 3 Nitrogen sorption isotherms (Top) and pore size distribution (PSD) curves for non-templated carbon aerogel (CAMF) before (inset) and after activation (12AC-CAMFX, where X is activation temperature) at KOH/carbon ratio = 2.

It is noteworthy that the sample activated at 600 °C is highly microporous with *ca.* 85% (*i.e.* 1272 $m^2 g^{-1}$) of the total surface area (*i.e.* 1504 $m^2 g^{-1}$) arising from micropores. The proportion of micropore surface area decreases to 24% after activation at 800 °C. Likewise the proportion of micropore volume decreases with increase in activation temperature from 72% at 600 °C to 14% at 800 °C. Thus, where necessary, templating may be combined with activation to further modify or optimise (with respect to surface area, microporosity or mesoporosity) the textural properties of the metal salt-templated carbon aerogels. To further clarify on the general applicability of metal salts as porogens, we are currently investigating a wide variety of metal salts. Early results indicate that not all soluble metal salts can act as porogens; for example we failed to generate porosity using $ZnCl_2$.

The CO_2 uptake capacity of the $CaCl_2$-templated carbon aerogels was determined at ambient temperature and pressure under flowing gas (pure CO_2) conditions. Table 1 summaries the CO_2 uptake of the carbons, which varies between 1.7 and 2.2 mmol g^{-1}. This is a significantly high uptake when considered against the surface area of the carbons as indicated by the uptake density of 1.7 to 2.7 μmol m^{-2}.[3,13] The relatively similar uptake despite the differences in textural properties indicates that the pore size distribution, which is comparable for all three sample, is likely an important variable in determining uptake. The CO_2 uptake as a function of time (Fig. S2, ESI†) indicates that the rate of uptake proceeds rapidly in the first few minutes and then gradually slows to a smooth increase as it approaches equilibrium. Maximum uptake is attained in *ca.* 50 min, which is comparable to what has previously been observed for porous carbons under similar conditions.[14] On the other hand, the CO_2 uptake of the activated non-templated carbon aerogels varied between 1 and 2 mmol g^{-1} (Table 2 and Fig. S3, ESI†), which is generally lower than that of the templated carbon aerogels. Thus in the present case, metal salt templating generates materials with overall superior properties for CO_2 uptake but *via* a much simpler and cheaper route. The kinetics of CO_2 uptake is also rather faster for the templated carbon aerogels compared to the activated non-templated carbons (Fig. S2 and S3, ESI†). These observations illustrate the potential of metal salt templating as an alternative to activation in generating carbon aerogels. Activation of the $CaCl_2$-templated carbon aerogel Ca-CAMF800, at 600 and 800 °C improves the CO_2 uptake capacity only slightly from 2.2 mmol g^{-1} to 2.5 and 2.6 mmol g^{-1}, respectively (Table S1, ESI†). It is however, clear that the increase in CO_2 uptake is proportionately lower than the rise in surface area after activation because most of the porosity generated during activation of the templated carbons is in the mesopore range and thus not efficient for CO_2 uptake.[4,15,16] The activated $CaCl_2$-templated carbons that have much higher surface may be more interesting for applications in hydrogen storage or as electrode materials for supercapacitors, which widens the potential appeal of the present carbon aerogels.[17]

In conclusion, we have demonstrated the successful metal salt-templated preparation of carbon aerogels *via* a simple subcritical drying route. The metal salt ($CaCl_2$) templating method offers an alternative to activation, especially where carbon aerogels with moderate surface area and pore volume are required. Furthermore, the templated carbon aerogels are amenable to activation to generate very high surface area carbons.

References

1 A. W. C. van den Bergm and C. O. Arean, *Chem. Commun.*, 2008, 668.
2 R. E. Morris and P. S. Wheatley, *Angew. Chem., Int. Ed.*, 2008, **47**, 4966.
3 Q. Wang, J. Luo, Z. Zhong and A. Borgna, *Energy Environ. Sci.*, 2011, **4**, 42.
4 S. Choi, J. H. Drese and C. W. Jones, *ChemSusChem*, 2009, **2**, 796.
5 (*a*) R. W. Pekala, *J. Mater. Sci.*, 1989, **24**, 3221; (*b*) F. M. Kong, J. D. LeMay, S. S. Hulsey, C. T. Alviso and R. W. Pekala, *J. Mater. Sci.*, 1993, **28**, 3100; (*c*) R. W. Pekala, *Macromolecules*, 1993, **26**, 5487.
6 (*a*) B. Mathieu, S. Blacher, R. Pirard, J. P. Pirard, B. Sahouli and F. Brouers, *J. Non-Cryst. Solids*, 1996, **212**, 250; (*b*) R. Kocklenberg, B. Mathieu, S. Blacher, R. Pirard, J. P. Pirard, R. Sobry and G. van den Bossche, *J. Non-Cryst. Solids*, 1998, **225**, 8; (*c*) H. Tamon, H. Ishizaka, T. Yamamoto and T. Suzuki, *Carbon*, 2000, **38**, 1099; (*d*) M. Mirzaeian and P. J. Hall, *Electrochim. Acta*, 2009, **54**, 7444.
7 (*a*) J. Biener, M. Stadermann, M. Suss, M. A. Worsley, M. M. Biener, K. A. Rose and T. F. Baumann, *Energy Environ. Sci.*, 2011, **4**, 656; (*b*) Y. Hanzawa, K. Kaneko, R. W. Pekala and M. S. Dresselhaus, *Langmuir*, 1996, **12**, 6167.
8 (*a*) R. W. Pekala, J. C. Farmer, C. T. Alviso, T. D. Tran, S. T. Mayer, J. M. Miller and B. Dunn, *J. Non-Cryst. Solids*, 1998, **225**, 74; (*b*) Z. Zapata-Benabithe, F. Carrasco-Marín and C. Moreno-Castilla, *J. Power Sources*, 2012, **219**, 80; (*c*) T. F. Baumann, M. A. Worsley, T. Y. J. Han and J. H. Satcher, *J. Non-Cryst. Solids*, 2008, **354**, 3513; (*d*) Y. S. Tao, M. Endo and K. Kaneko, *J. Am. Chem. Soc.*, 2009, **131**, 904; (*e*) R. Fu, T. F. Baumann, S. Cronin, G. Dresselhaus, M. S. Dresselhaus and J. H. Satcher, *Langmuir*, 2005, **21**, 2647; (*f*) H. Kabbour, T. F. Baumann, J. H. Satcher, A. Saulnier and C. C. Ahn, *Chem. Mater.*, 2006, **18**, 6087.
9 (*a*) Y. Xia, Z. Yang and R. Mokaya, *Nanoscale*, 2010, **2**, 639; (*b*) Y. Xia, G. S. Walker, D. M. Grant and R. Mokaya, *J. Am. Chem. Soc.*, 2009, **131**, 16493; (*c*) A. Almasoudi and R. Mokaya, *J. Mater. Chem.*, 2012, **22**, 146; (*d*) N. Alam and R. Mokaya, *Energy Environ. Sci.*, 2010, **3**, 1773; (*e*) Y. Xia and R. Mokaya, *J. Phys. Chem. C*, 2007, **111**, 10035; (*f*) Z. Yang, Y. Xia and R. Mokaya, *J. Am. Chem. Soc.*, 2007, **129**, 1673; (*g*) A. Pacula and R. Mokaya, *J. Phys. Chem. C*, 2008, **112**, 2764.
10 (*a*) C. Lin and J. A. Ritter, *Carbon*, 1997, **35**, 1271; (*b*) C. Lin and J. A. Ritter, *Carbon*, 2000, **38**, 849; (*c*) S. A. Al-Muhtaseb and J. A. Ritter, *Adv. Mater.*, 2003, **15**, 101; (*d*) E. Gallegos-Suárez, A. F. Pérez-Cadenas, F. J. Maldonado-Hódar and F. Carrasco-Marín, *Chem. Eng. J.*, 2012, **181**, 851.
11 K. S. W. Sing, D. H. Everett, R. A. W. Haul, L. Moscou, R. A. Pierotti, J. Rouquerol and T. Siemieniewska, *Pure Appl. Chem.*, 1985, **57**, 603–619.
12 (*a*) Y. Hanzawa, K. Kaneko, N. Yoshizawa, R. W. Pekala and M. S. Dresselhaus, *Adsorption*, 1998, **4**, 187; (*b*) T. Horikawa, Y. Ono, J. Hayashi and K. Muroyama, *Carbon*, 2004, **42**, 2683.
13 (*a*) G. P. Hao, W. C. Li and A. H. Lu, *J. Mater. Chem.*, 2011, **21**, 6447; (*b*) M. Sevilla, P. Valle-Vigon and A. B. Fuertes, *Adv. Funct.*

Mater., 2011, **21**, 2781; (*c*) Y. Xia, R. Mokaya, G. S. Walker and Y. Q. Zhu, *Adv. Energy Mater.*, 2011, **1**, 678; (*d*) L. Y. Meng and S. J. Park, *J. Colloid Interface Sci.*, 2010, **352**, 498; (*e*) T. C. Drage, A. Arenillas, K. M. Smith, C. Pevida, S. Piippo and C. E. Snape, *Fuel*, 2007, **86**, 22.

14 C. Pevida, T. C. Drage and C. E. Snape, *Carbon*, 2008, **46**, 1464.

15 Z. Zhang, J. Zhou, W. Xing, Q. Xue, Z. Yan, S. Zhuo and S. Z. Qiao, *Phys. Chem. Chem. Phys.*, 2013, **15**, 2523.

16 V. Presser, J. McDonough, S. H. Yeon and Y. Gogotsi, *Energy Environ. Sci.*, 2011, **4**, 3059.

17 (*a*) M. Sevilla, R. Mokaya and A. B. Fuertes, *Energy Environ. Sci.*, 2011, **4**, 2930; (*b*) M. Sevilla, A. B. Fuertes and R. Mokaya, *Energy Environ. Sci.*, 2011, **4**, 1400.